

# Challenges and Solutions in the Protection of Transmission Lines Connecting Nonconventional Power Sources

Marcelo Bini, *EDF Renewables*

Ricardo Abboud, Paulo Lima, and Fabio Lollo,  
*Schweitzer Engineering Laboratories, Inc.*

Revised edition released August 2023

Previously revised edition released January 2022

Originally presented at the  
48th Annual Western Protective Relay Conference, October 2021

# Challenges and Solutions in the Protection of Transmission Lines Connecting Nonconventional Power Sources

Marcelo Bini, *EDF Renewables*

Ricardo Abboud, Paulo Lima, and Fabio Lollo, *Schweitzer Engineering Laboratories, Inc.*

**Abstract**—This paper discusses the impact of inverter-based resources (IBRs) in traditional digital protection relays applied in the interconnection transmission line between the IBR and bulk power system. Real events involving a photovoltaic (PV) power plant are used to show the behavior of the fault currents, which is different from power systems with synchronous generators, especially for negative-sequence components. The paper discusses how to properly handle this kind of source by presenting modern protective relays features, time-domain functions, and special settings for traditional protection intelligent electronic devices (IEDs). The data of the real events were used to validate the solutions proposed in this case study. The lessons learned will be applied in a new facility (a wind farm) that is currently in the design stage.

## I. INTRODUCTION

Over the last decade, the renewable energy share of the electricity sector grew quickly. Renewable energy installations, especially solar photovoltaic (PV) facilities and wind turbines, are increasingly deployed today. The contribution of these sources to the power system affects the performance of conventional protection systems, particularly for faults on transmission lines that connect such power sources to the bulk power system. Most of these renewable power sources are inverter-based, and their characteristics change according to manufacturer design and specifications. The fault current contribution from an inverter-based resource (IBR) is limited by the current capacity of its power electronic components and its control functions. Typically, the maximum current capacity of these power components does not exceed 1.5 times the full-load current during the fault steady-state. Additionally, the IBRs do not have the same amount of rotational inertia as a synchronous generator [1]. Usually, the IBR does not deliver reliable negative-sequence and zero-sequence quantities, as the synchronous generators would do. The IBR's atypical behavior and characteristics challenge the phasor-based protective functions when compared to synchronous generators, because the assumptions made in their design are no longer valid, especially assumptions about the fault current contribution magnitude and associated negative-sequence behavior [1].

Numerical relay benefits and advantages are well known in the power industry, and the ease of obtaining the symmetrical components from the measured phase quantities is one of those advantages. It allows the implementation of several new functions based on symmetrical components, especially the negative-sequence component [2] [3] [4] [5] [6], since

obtaining the negative-sequence component in electromechanical and solid-state relays requires complex and more expensive analog filters [7] [8]. These new functions significantly improve the sensitivity, reliability, and security of transmission line protective functions and schemes, allowing for the secure detection of challenging line faults.

This paper evaluates how nonconventional power sources affect the security and reliability of phasor-based transmission line protection, especially the protective functions based on symmetrical components. First, the paper briefly reviews the short circuit contribution from nonconventional power sources, focusing on the IBRs. The paper reviews the main transmission line protective features based on negative-sequence components and their benefits in terms of sensitivity, reliability, and security.

A case study evaluating the performance of phasor-based protective features in a 138 kV transmission line connecting a 420 MW PV solar power plant to the bulk power system is presented. Data from real fault events in this transmission system are used to evaluate the line protective functions' performance.

The paper evaluates the performance of improved phasor-based and time-domain protective functions that are designed to provide reliable performance of the transmission line protection system connecting IBR to the grid. Data captured from real fault events are used to test and assess the effectiveness and performance of the improved phasor-based and time-domain protective features, and the results are presented and discussed.

Finally, the paper proposes protection philosophy combining phasor-based elements and time-domain incremental quantities. It is based on the validation made with field data in this paper and previous papers' conclusions. Possible modifications in the phasor-based function setting to improve security, as shown in [9], are also considered.

## II. IBR BEHAVIOR DURING POWER SYSTEM FAULTS

### A. Dynamic Behavior of Wind Turbines During Short Circuits

Wind turbines are complex systems that transform the kinetic energy of the wind into electrical energy, and wind generation is already responsible for a significant portion of the Brazilian energy matrix [10]. One of the specific features of wind generation is the high variability of wind strength, which

translates into variations in turbine rotations. For a generator, varying rotation means a varying generated signal frequency. Since there is a tendency for the frequency in the generator to vary and a simultaneous need to keep the frequency of the electrical system constant, several solutions have been developed to allow coupling between the wind turbine and the power system.

Wind turbines are commonly classified into different types, according to their operation and construction. Naturally, each type of generator contributes differently when there are faults in the system. There are many studies that seek to find the best way to model the different types of machines to understand their behavior during system faults [11]. Good modeling allows users to feel more confident when calculating generator contributions for short circuit and yard equipment strength studies.

References [12] and [13] present the Type I and Type II wind turbine characteristics and fault contributions, respectively. The contributions of Type III generators during faults can be divided into two behaviors, which depend on whether or not the crowbar is active. When the crowbar is active, the power electronics do not control the field winding; therefore, the behavior is similar to that of the induction generator. Also, when the generator with the activated crowbar is contributing, some components can have frequencies other than nominal frequency, since the axis rotation of the machine is not necessarily in sync with the network. The highest short circuit levels of the Type III wind turbine are obtained when the crowbar is active [14].

When the crowbar is not active and the network is under fault conditions, wind turbine contributions are determined by the power electronics. In this situation, the control network developed by the manufacturer is largely responsible for determining the dynamic response of the machine. We have seen different responses among different manufacturers and different wind turbines from the same manufacturer.

Type IV has its short circuit current fully controlled by the power electronics. These devices are sized to carry a current level slightly above the nominal current, which limits the contribution of these generators to a range of 1.1 to 1.3 pu of the nominal current for most of the time [1] [15]. Another characteristic is the low capacity to supply negative-sequence current; the short circuit current of this type of generator tends to be balanced, even for unbalanced faults.

### B. Behavior of PV Power Plants During Short Circuits

Generation of electrical energy through PV panels involves converting sunlight into electrical energy. This conversion occurs due to the semiconductor characteristics of the material (normally silicon), which is used in PV cells due to its commonality.

The PV modules are composed of a set of interconnected solar cells that transform energy. The cell connections are directly related to the voltage and electric current that the module needs to supply to comply with the manufacturing design [16].

PV generation systems consist of the connection of solar modules in series, in parallel, or as a combination of the two in which each string is made up of a certain number of modules to obtain the desired voltage and current levels. Generally, power is the technical specification most used to classify PV modules, and the unit widely used is peak watt (Wp).

The complete system of a solar plant, at the generation level, is composed of the following equipment:

- Solar modules
- Combiner box
- Inverter
- Step-up transformer

To produce the necessary power, the solar modules are interconnected and form strings. These strings are brought together in a combiner box, and the outputs of the combiner box are connected to the ac/dc inverters, which convert the dc voltage to ac voltage using a three-phase rectifier. The outputs of the inverters are linked to step-up transformers to connect the energy at medium voltage level to a collector substation, which then raises the voltage to make the generated energy available through the power system.

Grid-connected solar power plants contribute to short circuit currents during a fault, modifying the short circuit characteristic in the power system. The contribution to the short circuit current depends on a variety of factors, including the maximum current level supported by the inverter, inverter control systems, environmental conditions, protection system, location, and type of fault.

## III. FIELD CASE ANALYSIS

Fig. 1 shows the main features of the system used as a case study. The field case study is based on a solar PV power plant located in Brazil, which has an installed capacity of approximately 420 MW. The PV is connected to Brazil's national interconnected system (GRID) through three three-winding step-up transformers, as shown in Fig. 1:

- 34.5 kV sector—PV distribution voltage level with resistance-grounded and Y-connected step-up transformer winding. The inverters are connected to the 34.5 kV bus through 0.38/34.5 kV step-up transformers, not shown in Fig. 1.
- 138 kV sector—PV transmission voltage level with solid-grounded and Y-connected transformer winding for connection to the GRID through the 138 kV transmission line with a length of 10.37 km (6.44 miles).
- Delta (D) tertiary winding for harmonic filtering with no load connected.

The transmission line in analysis has protective relays installed at both terminals, indicated in the diagram as IED\_PV and IED\_GRID.

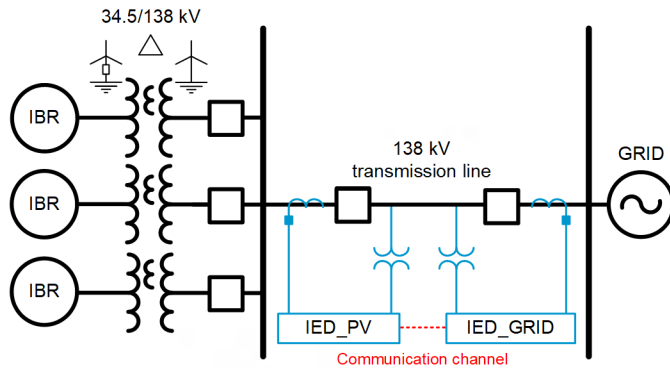


Fig. 1. Simplified single-line diagram of the PV used in the case study.

The applied intelligent electronic device (IED) is a transmission line protective relay, and the main enabled functions for circuit breaker (CB) tripping are as follows:

- Line differential protection—phase elements (87LA, 87LB and 87LC), negative-sequence element (87LQ), and zero-sequence element (87LG) are enabled
- Phase and ground distance time-delayed elements (Z2T)—Zone 1 is not enabled due to short line length and PV fault contribution behavior
- Directional comparison teleprotection scheme with permissive overreach transfer trip (POTT) by overreaching distance (Z2) and neutral directional overcurrent (67G2) element
- Direct transfer trip (DTT)
- Emergency overcurrent protection (51E)—only enabled in case of simultaneous loss-of-potential and loss of differential channel communications
- Phase overvoltage protection (59P)

There is an AG fault in the grid, outside the 138 kV interconnection transmission line. At the time of the fault, the PV is connected generating energy; therefore, there is a contribution from the PV to the fault.

Fig. 2 shows the currents and voltages during the AG fault external to the transmission line. Users can conclude that it is an AG short circuit due to the voltage sag in the A-phase and the current increase in this phase at the beginning of the short circuit. Current increases in the other phases and distortions in the waveforms are a challenge for the protection schemes that are currently employed.

For this fault, the 138 kV line protection should not cause the opening of CBs. However, as Fig. 2 shows, the IED\_GRID trips (2:TRIP). The current flowing through the IEDs at both line terminals is the contribution of the PV, which has high distortion and is not consistent with the contribution of a synchronous machine to an AG fault.

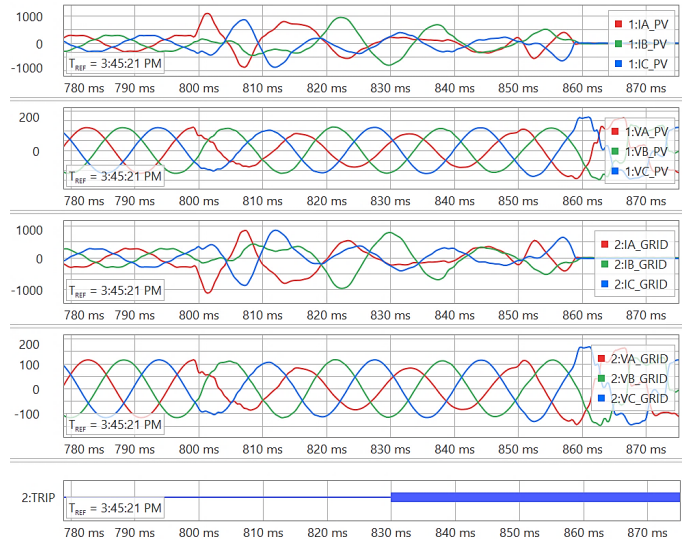


Fig. 2. Oscillography records with current (amperes), voltage (kilovolts), and digital signals from the PV and GRID terminals for the external AG fault.

The small dip in the A-phase voltage suggests that it was a short circuit in the grid relatively distant (electrically) from the transmission line in question. Field personnel reports that the fault occurred approximately 200 km (124 miles) away from the transmission line in question.

Fig. 3 shows the waveforms for each phase and both terminals separately. This makes it easy to observe that the current entering the line through the PV terminal is equal to the current leaving the line through the GRID terminal (the currents from both sides are in opposition of phase). This proves that it was an external fault to the line.

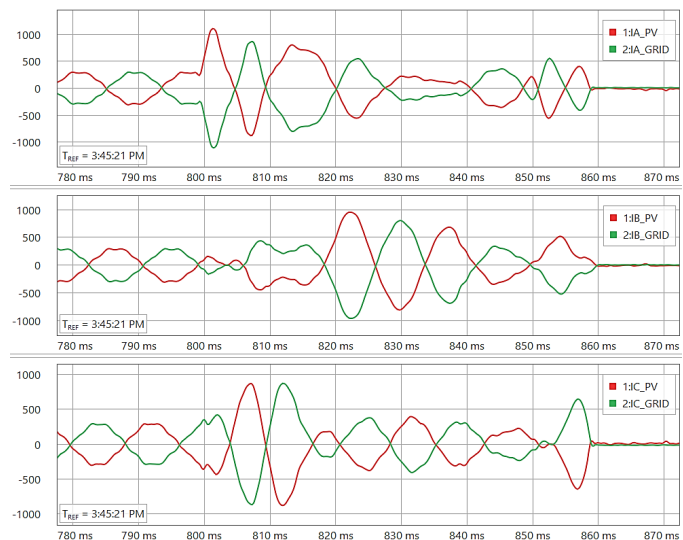


Fig. 3. Currents by phase (amperes) at both line terminals.

The rest of this paper provides a more detailed analysis of the behavior of the protection functions during this event.

### A. Fault-Type Identification Logic

In faults involving the ground, the protection IEDs compare the negative-sequence current ( $I_2$ ) and zero-sequence current ( $I_0$ ) phasors to identify which type of fault is occurring in the system. Using the A-phase as a reference for calculating the symmetrical components for an AG or BCG (FSA) fault,  $IA_2$  and  $IA_0$  are expected to be in-phase. For a BG or CAG (FSB) fault,  $IA_2$  is expected to lag  $IA_0$  by 120 degrees, and for a CG or ABG (FSC) fault,  $IA_2$  is expected to lead  $IA_0$  by 120 degrees. Fig. 4 shows these expected relationships. To identify whether the fault is single-phase or two-phase to the ground, a comparison is made between the apparent impedance of the respective fault loops. The one with the lowest apparent impedance is the fault loop [6].

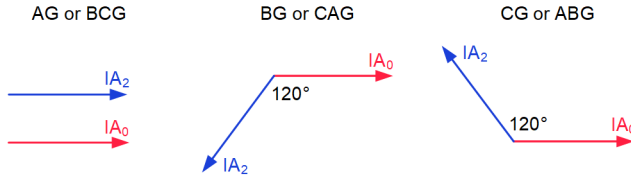


Fig. 4. Relationship between  $I_2$  and  $I_0$  for AG, BG, CG, BCG, CAG, and ABG faults.

In the event analyzed,  $I_2$  has unstable behavior, as seen in Fig. 5, which shows the filtered current and voltages at the GRID terminal. This same behavior occurs at both transmission line terminals, since the PV fault current contribution passes through both terminals, as also reported in [1].

After adopting the A-phase voltage (VA) as the angular reference, the following  $I_2$  behavior is observed during the event:

- At the beginning of the fault,  $I_2$  is in-phase with  $I_0$ , a characteristic behavior of an AG or BCG fault (Fig. 5a).
- At the middle of the fault,  $I_2$  leads  $I_0$  by approximately 120 degrees, a characteristic behavior of a CG or ABG fault (Fig. 5b).
- At the end of the fault,  $I_2$  lags  $I_0$  by approximately 140 degrees, a characteristic behavior of a BG or CAG fault (Fig. 5c).

$I_0$  remains stable in respect to VA throughout the fault, with an angular difference compatible with an AG fault. The D-winding of the 34.5/138 kV step-up transformers in the PV provides a low-impedance path for the zero-sequence current, and this causes the GRID to contribute a portion of the  $I_0$  current that flows in the direction from the PV to the GRID. Thus,  $I_0$  is less dependent on the behavior of the inverters and has a more predictable behavior in this type of system, given that the GRID has mostly conventional sources. Fig. 5 also shows the response of the faulted phase selection logic at the GRID terminal for this event.

This unexpected behavior of the relationship between  $I_2$  and  $I_0$  leads relays that use this methodology to misidentify the fault type and enable unsuitable fault loops. This can have consequences, such as underreaching or overreaching distance protection, errors in the fault-locating function, and incorrect openings in cases when single-pole tripping is applied.

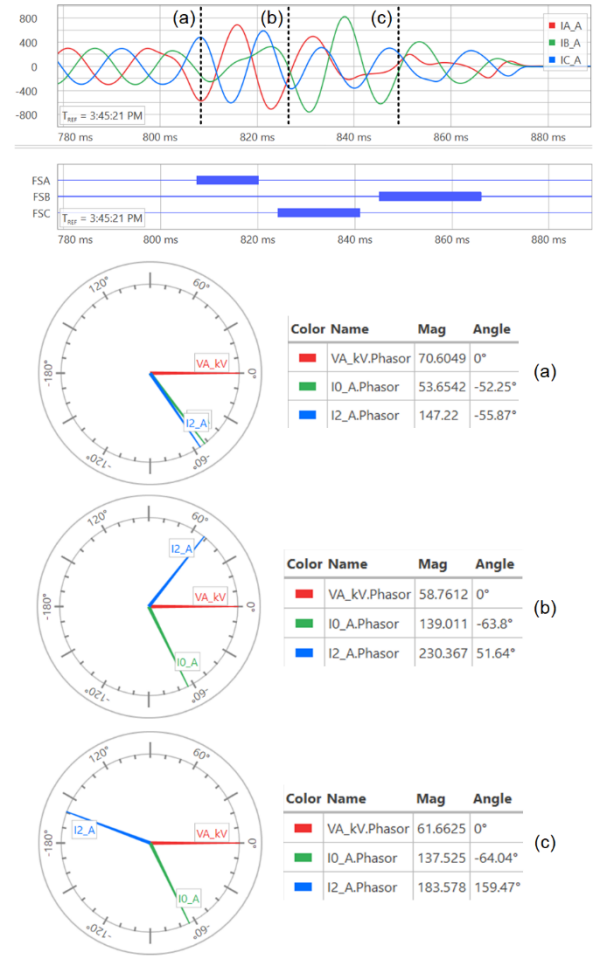


Fig. 5. Fault current (amperes) and behavior of  $I_2$  in relation to  $I_0$  during AG fault in the system, studied at different times during the fault.

Reference [6] fully describes a modern implementation of fault-type identification and how incorrect selection affects the safety and reliability of protection functions.

### B. POTT

The GRID terminal circuit breaker is tripped by the POTT scheme. Fig. 6 shows the currents of both terminals with indications of the digital elements of both IEDs.

The IED\_PV initially sees the fault as forward (1:32GF) and transfers the permissive signal to the GRID terminal (1:KEY). In relation to the PV terminal, the fault is actually in the forward direction.

The IED\_GRID receives the permissive signal from the PV terminal (2:PT) and, when it sees the fault directionality as forward (2:32GF), it issues a tripping command via the POTT scheme (2:TRPRM). For the GRID terminal, the fault should be declared as reverse.

Despite initially having declared the fault as forward (1:32GF), the IED\_PV starts to define the fault as reverse (1:32GR) at approximately 830 ms, at the same time that the IED\_GRID defines the fault as forward (2:32GF). We will analyze what caused this behavior with further details. The negative-sequence directional element (32Q) was set to provide directional decisions for the residual ground directional

overcurrent element (67G2), and this was the element responsible for the POTT scheme operation.

In a traditional negative-sequence directional element, the angular relationship between the negative-sequence voltage ( $V_2$  and  $I_2$ ) determines the fault direction. For a forward fault,  $I_2 \cdot 1 < Z_L \text{ANG}$  ( $I_{2R}$ ) is expected to be 180 degrees out with  $V_2$ ; whereas, the reverse fault  $I_{2R}$  is expected to be in-phase with  $V_2$  [17], as shown in Fig. 7. When setting  $V_2$  as the angular reference,  $I_{2R}$  is expected to be in the blue region for forward faults and in the red region for reverse faults. The region in black is where the direction is undefined.

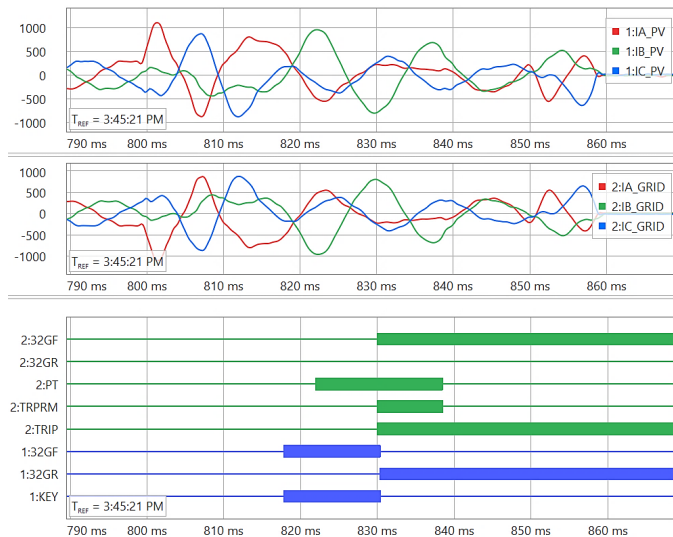


Fig. 6. Oscillography records with current signals (amperes) and indications of the protections activated on the PV and GRID terminals for the external AG fault.

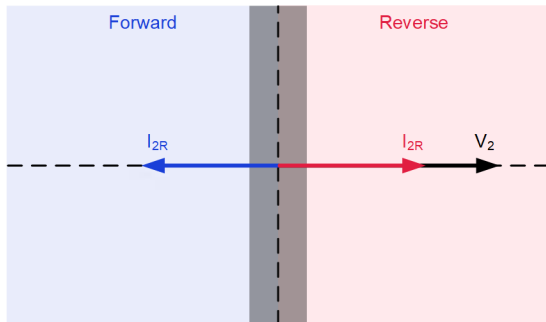


Fig. 7. Relationship between  $V_2$  and  $I_{2R}$  for forward and reverse faults.

The protection IEDs used in the analyzed line have a 32Q element based on measuring the negative-sequence impedance [18]. For a forward fault, the relationship between  $V_2$  and  $I_2$  is the negative sequence of the source impedance ( $-Z_S$ ), as shown in Fig. 8a. For a reverse fault, the relationship between  $V_2$  and  $I_2$  is the sum of the line impedance and the remote source impedance ( $Z_L + Z_R$ ), as shown in Fig. 8b [1].

Here, we will use only the relationship between  $V_2$  and  $I_{2R}$  to simplify the analysis. For the IED\_PV, at the beginning of the fault, the relationship between  $I_{2R}$  and  $V_2$  is consistent with a forward fault but very close to the undefined direction (shown in Fig. 9a). However, at a later time, the relationship between

$I_{2R}$  and  $V_2$  indicates a clear reverse fault (shown in Fig. 9b), justifying the change of directionality determined by this relay.

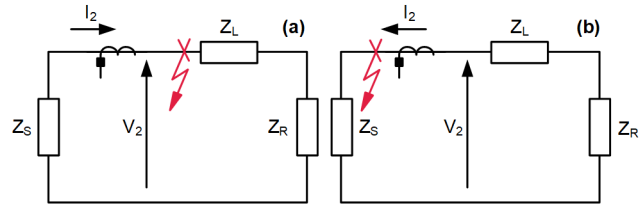


Fig. 8. Operating principles of element 32Q during a forward fault (a) and during a reverse fault (b).

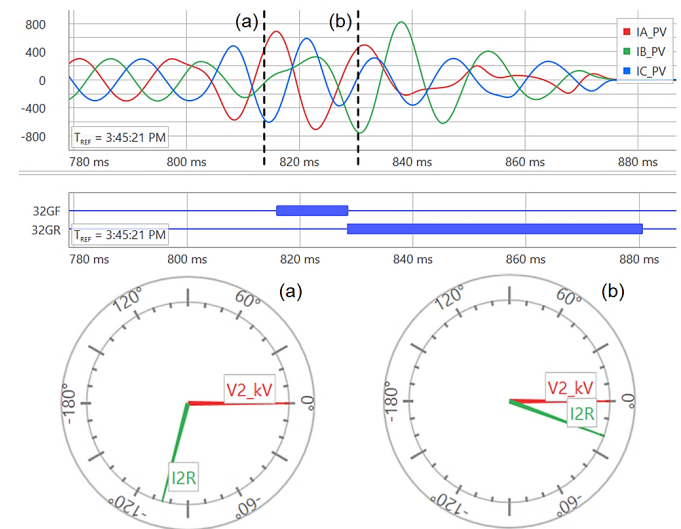


Fig. 9. Fault current (amperes) and relationship between  $I_{2R}$  and  $V_2$  for the IED\_PV at different times during the fault.

For the IED\_GRID, at the beginning of the fault, the relationship between  $I_{2R}$  and  $V_2$  is in an undefined region, and the IED did not determine the fault to be in either direction (shown in Fig. 10a). At a later time, the relationship between  $I_{2R}$  and  $V_2$  indicates a forward fault condition (shown in Fig. 10b), justifying the IED's determination that the direction of the fault was forward.

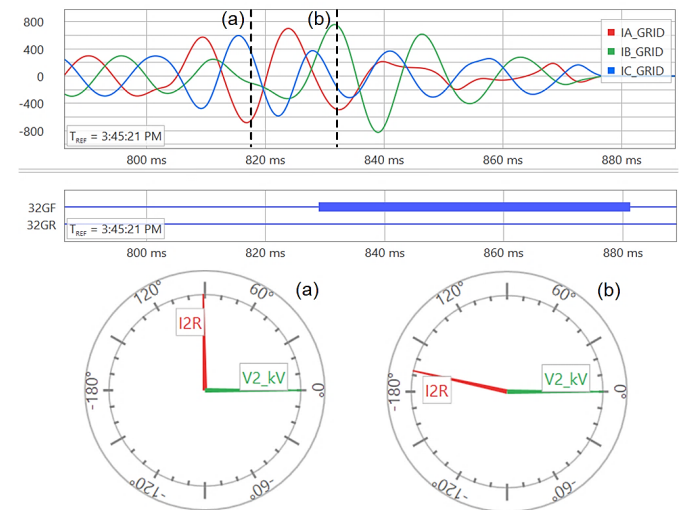


Fig. 10. Fault current (amperes) and relationship between  $I_{2R}$  and  $V_2$  for the IED\_GRID at different times during the fault.

A similar analysis can be performed to assess how a directional element would behave based on zero-sequence current ( $I_0$ ) and zero-sequence voltage ( $V_0$ ). The same diagram can be used for this (shown in Fig. 7) if  $V_2$  is replaced with  $V_0$  and  $I_2R$  is replaced with  $I_0R$ . The IED in question has a directional element based on the measurement of the zero-sequence impedance (32V); its operational principle is similar to that of the 32Q element (shown in Fig. 8).

Fig. 11 shows that at the PV terminal, the angular relationship between  $I_0R$  and  $V_0$  is compatible with a forward fault, and the relationship remains this way throughout the fault.

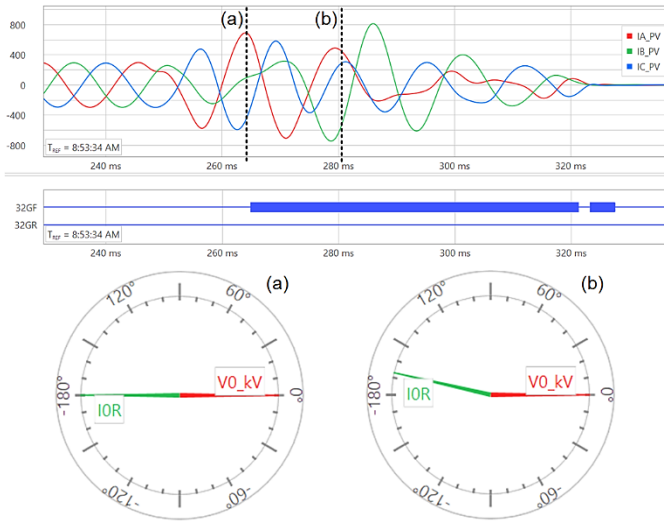


Fig. 11. Fault current (amperes) and relationship between  $V_0$  and  $I_0R$  for the IED\_PV at different times during the fault.

Fig. 12 shows that at the GRID terminal, the angular relationship between  $I_{0R}$  and  $V_0$  is compatible with a fault in the reverse direction, and the relationship remains this way throughout the fault. This stable, predictable behavior of zero-sequence quantities shows that in this type of system, these quantities are more appropriate than negative-sequence quantities. This is mainly due to the connection of the PV transformers, which allow the system to contribute zero-sequence through the PV terminal. In other words, the zero-sequence that mostly passes through the PV terminal during an external fault is actually contributed by the system and not by the inverters.

For this particular case,  $I_0R$ - and  $V_0$ -based directional elements are shown to be reliable; however, in some applications, like in parallel lines, the zero-sequence mutual coupling can be a challenge when applying the zero-sequence directional element. The negative-sequence directional element has always been the natural choice of protection engineers in these cases [3] [17].

Additionally, the negative-sequence directional element is the main method for determining the directionality of unbalanced faults between phases and is used to supervise phase overcurrent elements and phase distance elements in traditional phasor-based implementations [18].

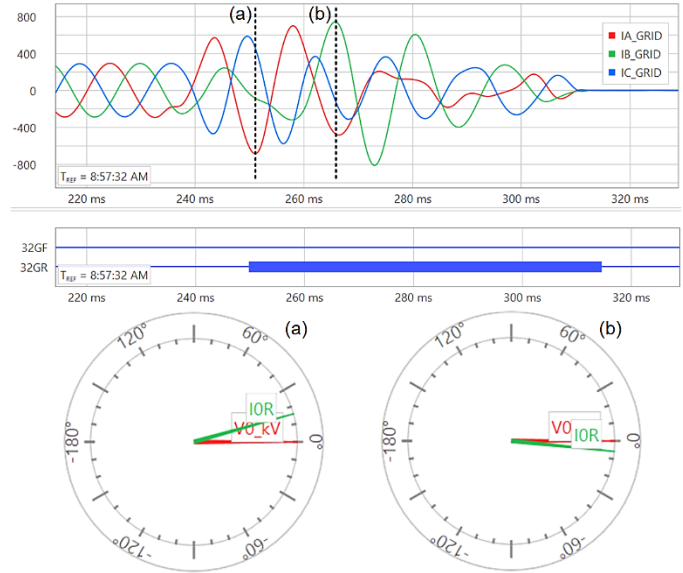


Fig. 12. Fault current (amperes) and relationship between  $V_0$  and  $I_0R$  for the IED\_GRID at different times during the fault.

The protection of transmission lines in the vicinity of unconventional sources results in an additional complication and may leave protection engineers without a reliable alternative for determining the directionality of faults.

### C. Line Differential Protection Element (87L)

The applied IED has a line differential element (87L) with an alpha plane operating principle [19] and provides the phase differential elements (87LA, 87LB and 87LC), negative-sequence element (87LQ), and zero-sequence element (87LG).

Fig. 13 shows the filtered phase, negative-sequence, and zero-sequence currents measured at each line terminal, as well as the respective differential current. The currents recorded at each terminal have the same magnitude and a 180 degrees difference, resulting in a differential current that equals zero.

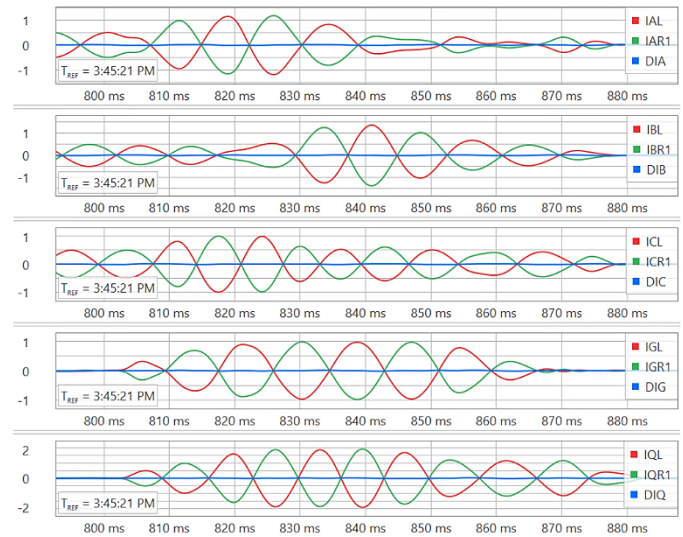


Fig. 13. Filtered phase, negative-sequence, and zero-sequence currents (in per unit) measured at each line terminal.

In the external fault condition, despite the unstable behavior of the unconventional source, its contribution is a current passing through the line; therefore, this does not cause a differential current in the phase, negative-sequence, and zero-sequence elements.

For an internal fault in the protected line, the IED at the GRID terminal measures the current contributed by the system, while the IED at the PV terminal measures the current contributed by the PV plant. This is not a problem for the phase and zero-sequence differential elements, given the characteristics of the system. For the negative-sequence differential element, it is not a problem at first, since the contribution of the GRID is significantly greater than the contribution of the PV. As this paper is being written, no internal fault events on the line are available for analysis. Considering that the contribution to an internal fault at the GRID terminal is much greater than that at the PV terminal, the 87LQ element will also operate reliably under unbalanced internal faults.

#### D. Distance Element (21)

There was no distance element pickup for this event because the fault was far from the protected line. Fig. 14 shows the Mho Zone 2 element characteristic and AG loop apparent impedance. During the fault, the apparent impedance varies greatly.

In the case where the fault is within the overreaching zone, this variation in apparent impedance during the fault could cause the apparent impedance to move in and out of the zone, preventing the element from operating and acting as a backup for external faults in the system. References [1] and [20] show how the behavior of unconventional sources affects distance relays.

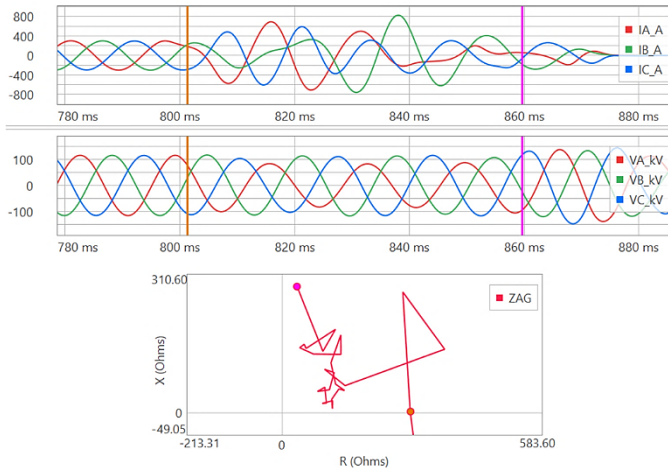


Fig. 14. Fault current (amperes), voltage (kilovolts), and behavior of the Mho Zone 2 and AG loop apparent impedance for the external AG fault.

## IV. EVALUATION OF NEW PROTECTIVE FEATURES

In this section, the performance of new protection functions for events in the system is evaluated. Both phasor-based protection functions were modified to better adapt to the contribution of IBRs to faults, and new time-domain-based functions are evaluated.

#### A. Incremental-Quantity Directional Element (TD32)

Reference [21] demonstrates the operational principle of the TD32 element, which operates based on the incremental voltage ( $\Delta v$ ) and the incremental replica current ( $\Delta i_Z$ ).

For a forward fault, the relationship between  $\Delta v$  and  $\Delta i_Z$  is the negative of the absolute value of the source impedance behind the relay ( $Z_S$ ), according to (1).

$$\Delta v = -|Z_S| \cdot \Delta i_Z \quad (1)$$

For a reverse fault, the relationship between  $\Delta v$  and  $\Delta i_Z$  is the absolute value of the sum of the protected line impedance ( $Z_L$ ) with the source impedance of the remote terminal ( $Z_R$ ), according to (2).

$$\Delta v = |Z_L + Z_R| \cdot \Delta i_Z \quad (2)$$

The graphical representation of  $\Delta v$  and  $\Delta i_Z$  during system faults helps us understand how the relationship between these quantities indicates the fault direction (shown in Fig. 15) [21].

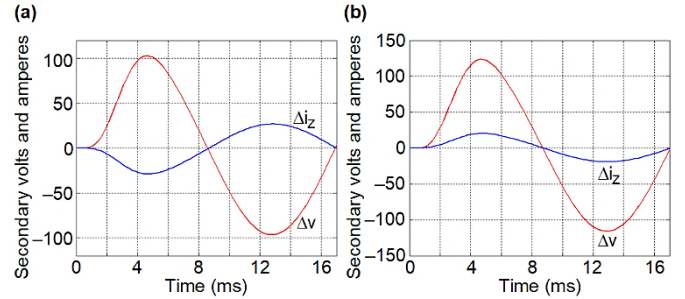


Fig. 15. Incremental voltage and incremental replica current for a forward fault (a) and for a reverse fault (b).

After observing Fig. 15, we can conclude that the incremental voltage and the incremental replica current have similar waveforms and that the relationship between their polarities clearly indicates the fault direction: quantities have an opposite polarity for forward faults, and quantities are in-phase for reverse faults. Additionally, the relationship between their magnitudes is related to the system impedances. Reference [21] details the implementation of the high-speed TD32 element, based on the relationship between  $\Delta v$  and  $\Delta i_Z$ .

The next section evaluates the performance of the TD32 element during the events in the system under study. To do this, we will play back the real field events in an IED with the TD32 function implemented [22].

### 1) Case 1: External AG Fault

This is the same fault assessed in Section III. Fig. 16 shows the behavior of the incremental voltage and incremental replica current at the PV terminal for the external AG fault. As expected, at the beginning of the fault, these quantities have opposite polarities, and the relay classifies the fault as forward (TD32F = 1).

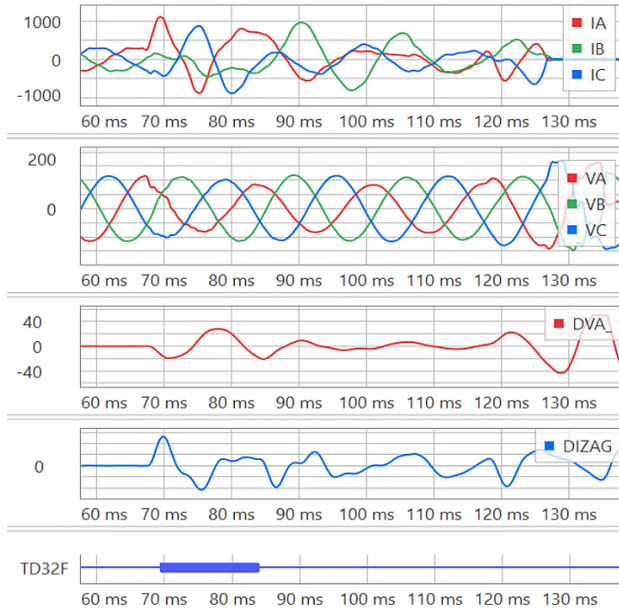


Fig. 16. Fault current (amperes), voltage (kilovolts), incremental voltage (kilovolts), and incremental replica current (amperes) at the PV terminal for an external AG fault.

Fig. 17 shows the behavior of the incremental voltage and incremental replica current at the GRID terminal for the external AG fault. As expected, at the beginning of the fault, these quantities have the same polarity, and the relay classifies the fault as reverse (TD32R = 1).

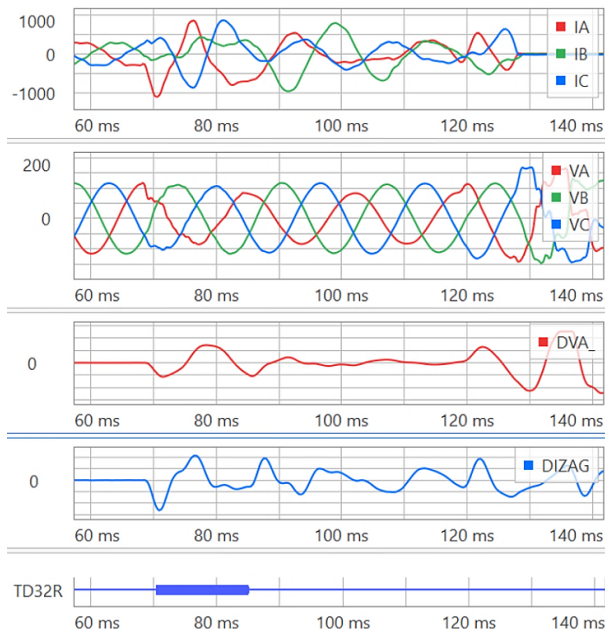


Fig. 17. Fault current (amperes), voltage (kilovolts), incremental voltage (kilovolts), and incremental replica current (amperes) at the GRID terminal for an external AG fault.

### 2) Case 2: External BG Fault Without Power Generation at PV

This external BG fault represents a condition different from the external AG fault described previously, since it occurred at a time when the PV had zero generation. Thus, the only current contribution to the fault was the zero-sequence current of the system through the transformers at the PV terminal. Additionally, this fault is much closer to the protected line than the previous fault.

Fig. 18 shows the behavior of the incremental voltage and incremental replica current at the PV terminal for this fault. As expected, at the beginning of the fault, these quantities have opposite polarities, and the relay reliably classifies the fault as forward (TD32F = 1).

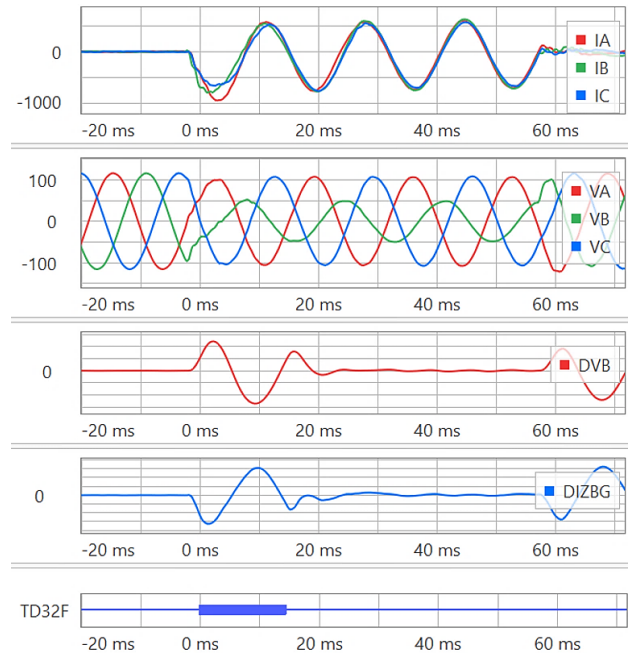


Fig. 18. Fault current (amperes), voltage (kilovolts), incremental voltage (kilovolts), and incremental replica current (amperes) at the PV terminal for an external BG fault.

Fig. 19 shows the behavior of the incremental voltage and incremental replica current at the GRID terminal for this fault. As expected, at the beginning of the fault, these quantities are in-phase, and the relay reliably classifies the fault as reverse (TD32R = 1).

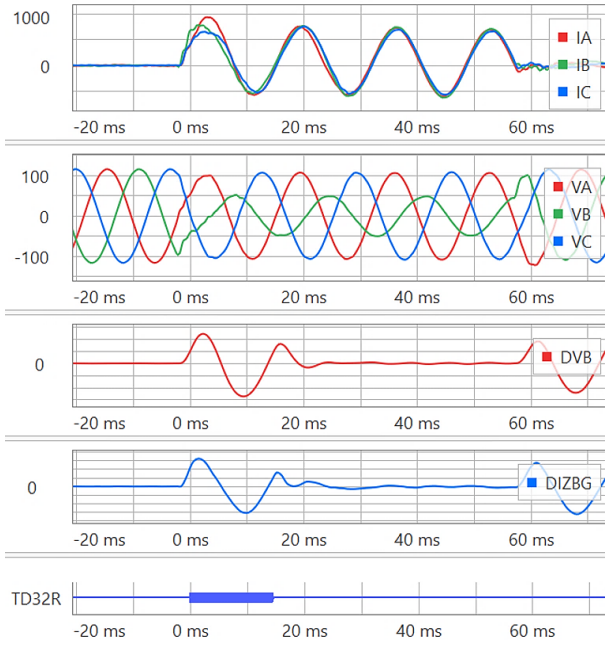


Fig. 19. Current (amperes), voltage (kilovolts), incremental voltage (kilovolts), and incremental replica current (amperes) at the GRID terminal for an external BG fault.

The operational situation described in this case is quite common, because it is a solar plant and there is no energy generation at night.

Reference [17] shows how this kind of fault with only zero-sequence current can cause improper operation of directional elements with a traditional quadrature connection; this is more critical, specifically in short lines, because the high zero-sequence current can reach the phase directional overcurrent element pickup level. Both the TD32 element and the 32V element shown previously are safe for this type of fault.

At the time of writing this paper, we only have faults involving the ground to evaluate the performance of the TD32 element; however, [20] considers the use of TD32 reliable for all fault types in this kind of application.

#### B. *Traveling-Wave (TW) Differential (TW87) and TW Directional (TW32) Elements*

Reference [21] describes the principles and fundamentals of protection functions based on current and voltage TWs, namely TW32 and TW87.

These elements operate based on the high frequency transient signals generated by the fault and are independent of the source's contribution to the fault in the first place. Thus, these elements are alternatives for protecting lines where one or more terminals have IBR connected.

This paper does not intend to evaluate the performance of these elements, since there are no high frequency sampled records on the order of MHz available in the system evaluated here.

#### C. *Enhanced Phasor-Based and Incremental-Quantity Fault-Type Identification Logics*

The IED of [22] implements a faulted phase selection logic based on incremental quantities. This logic is important for supervising protection elements based on incremental quantities, such as the TD32 element and the underreaching distance element based on incremental quantities (TD21) [23].

For pilot protection with single-pole trip schemes, the correct identification of the phase under fault is also needed to trip the correct phase. This logic based on incremental quantities is used in [22] in pilot protection schemes based on TD32, TD21, and TW32.

As shown previously, the elements based on incremental quantities behaved properly during real faults in the system under study. These functions can be safely applied to perform fast tripping for internal faults in the protected transmission line.

However, the incremental quantities are available for a limited time after the fault begins. This time is determined by the number of periods used in the calculation of the incremental quantity [21]. Thus, these functions do not provide backup protection for external faults in the system, similar to 87L function. Hence, the protection system must be complemented with phasor-based functions.

One of the challenges described in Section III for phasor protection is the correct identification of the phase under fault due to the unexpected behavior of the symmetrical components in the contribution of the IBR.

The IED of [22] also implements phasor-based fault-type identification logic (FID) that uses the negative- and zero-sequence voltages in addition to the negative and zero-sequence currents. The objective of using sequence voltages is to allow the FID logic to operate reliably under weak infeed conditions or when sequence currents are small and unreliable, as in the case of IBRs [22]. The logic calculates two quantities, as seen in (3) and (4).

$$S_2 = 3I_2 \cdot 1\angle Z1ANG - H_2 \cdot 3V_2 \quad (3)$$

$$S_0 = 3I_0 \cdot 1\angle Z1ANG - H_0 \cdot 3V_0 \quad (4)$$

where:

$3I_2$  is the negative-sequence current

$3I_0$  is the zero-sequence current

$Z1ANG$  is the positive-sequence line impedance angle

$3V_2$  is the negative-sequence voltage

$3V_0$  is the zero-sequence voltage

$S_2$  is the negative-sequence quantity

$S_0$  is the zero-sequence quantity

$H_2$  and  $H_0$  are constants

In addition to  $S_2$  and  $S_0$ , the logic also uses the positive-sequence voltage ( $V_1$ ) in determining the fault type when there is no ground involved and also to determine whether the fault is, for example, CG or ABG. Fig. 20 shows the expected angular relationship between these quantities for each fault type [22]. In Fig. 20, the fault is BCG, confirmed both by the relationship between  $S_0$  and  $S_2$  and by the relationship between  $S_2$  and  $V_1$ .

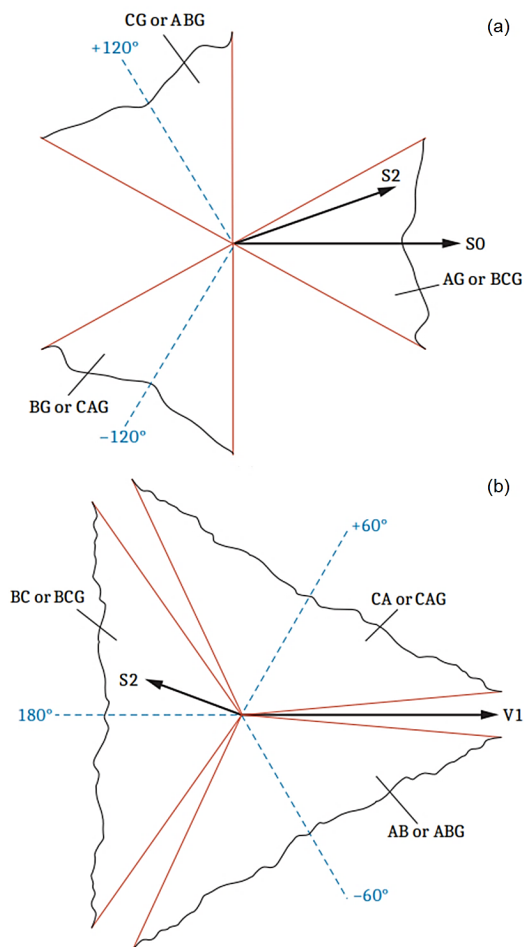


Fig. 20. The relationship between  $S_0$  and  $S_2$  (a) and the relationship between  $S_2$  and  $V_1$  (b) during unbalanced faults.

In [22], this logic is used for improved identification of phase under fault and is used in the following applications:

- To allow single-pole tripping in pilot protection schemes with 67G and 67Q
- To allow single-pole tripping in the pilot protection scheme using weak infeed logic with 59G and 59Q
- To improve fault-type signaling
- To improve fault-type selection for the impedance-based fault-locating function
- To improve single-pole tripping in DTT schemes without phase-separated bits

Given the applications and operating principle of this logic, it should work for faults in the forward direction.

We evaluated the performance of the improved phasor-based fault-type identification logic and the incremental-quantity-based faulted phase selection logic for the events in Case 1 and Case 2, presented above.

In Fig. 21, events marked with “1” are from the GRID terminal and those marked with “2” are from the PV terminal. The IED of the PV terminal correctly identifies the fault as AG by using the improved phasor-based element (2:FIDAG) and using the element based on incremental quantities (2:FSAG). The IED of the GRID terminal correctly identifies the fault using the element based on incremental quantities (1:FSAG), and there is no indication of using the improved phasor element (1:FIDAG), as expected, since the fault is in the reverse direction.

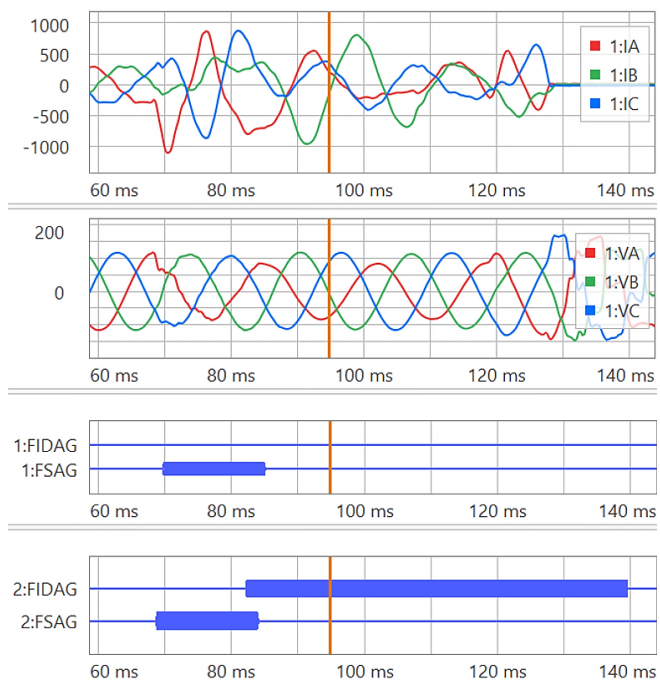


Fig. 21. Fault current (amperes), voltage (kilovolts), performance of the improved phasor-based faulted phase selection logic (1:FIDAG and 2:FIDAG), and the incremental-quantity-based faulted phase selection logic (1:FSAG and 2:FSAG) for Case 1.

For Case 2, the PV terminal IED correctly identifies the fault as BG by using the improved phasor-based element (2:FIDBG) and using the incremental-quantity-based element (2:FSBG), as shown in Fig. 22. The IED of the GRID terminal correctly identifies the fault using the incremental-quantity-based element (1:FSBG), and there was no indication of using the improved phasor-based element (1:FIDBG), as expected, as the fault is in the reverse direction for this line end.

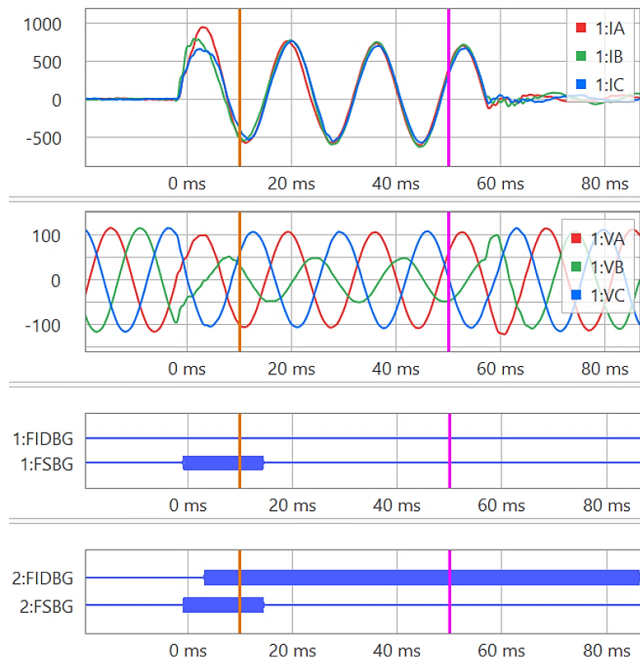


Fig. 22. Fault current (amperes), voltage (kilovolts), performance of the improved phasor-based faulted phase selection logic (1:FIDBG and 2:FIDBG), and the incremental-quantity-based faulted phase selection logic (1:FSBG and 2:FSBG) for Case 2.

Fig. 23 shows the performance of the faulted phase selection logic for a CAG fault external to the protected line. For this case, only the PV event is available. Both logic options correctly identify the phases under fault. Additionally, the correct behavior of the TD32 element is shown.

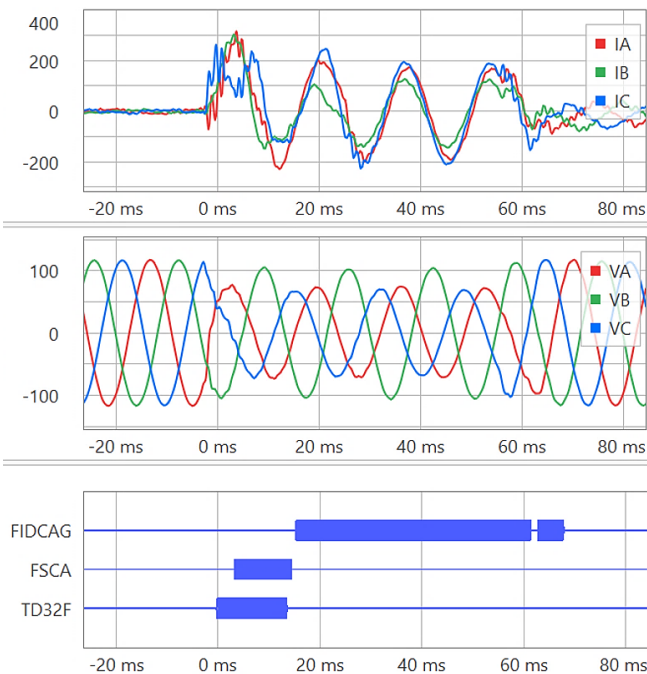


Fig. 23. Fault current (amperes), voltage (kilovolts), performance of the improved phasor-based faulted phase selection logic (FIDCAG), incremental-quantity-based faulted phase selection logic (FSCA), and TD32F for an external CAG fault.

The improved method described was proven to be safer and more robust than the traditional method based only on symmetrical component currents in the events evaluated.

## V. LINE PROTECTION SYSTEM CONFIGURATION FOR THE NEW WIND FARM ENTERPRISE

A new wind farm is being built, which will connect to the national interconnected system (GRID) through a single-circuit, 500 kV overhead transmission line with a length of 27 km (16.8 mi).

This section discusses how the new protection system for this transmission line is being designed. Given the experience protecting the 138 kV transmission line at the PV and the performance available using the new protection elements described in Section IV, a relay that combines time-domain with phasor-based features was chosen for the Main 1 protection and a phasor-based line differential relay was chosen for the Main 2 protection of this new transmission line.

Fig. 24 shows the simplified single-line diagram of the wind farm and its connection with GRID.

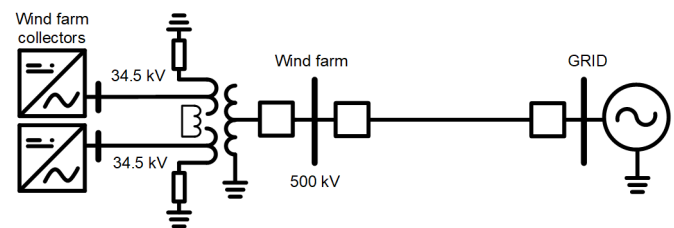


Fig. 24. Simplified single-line diagram of new EDF Renewables wind farm and its connection with GRID.

### A. Pilot Protection Scheme

The transmission lines connecting the wind farm with GRID have an optical ground wire (OPGW). The POTT pilot protection scheme will be adopted.

The following directional elements are available:

- Main 1 protection IED
  - Directional element based on incremental quantities (TD32)
  - Directional element based on TWs (TW32)
  - Negative-sequence impedance directional element (32Q)
  - Zero-sequence impedance directional element (32V)
  - Phase directional element (32P-1)
- Main 2 protection IED
  - Negative-sequence impedance directional element (32Q)
  - Zero-sequence impedance directional element (32V)
  - Phase directional element (32P-2)

The phase directional elements (32P) in each IED are classified with different codes as they have different operating principles:

- 32P-1—phase directional element polarized with positive-sequence voltage memory
- 32P-2—phase directional element based on the positive-sequence impedance angle, obtained from the relationship between the positive-sequence voltage and positive-sequence current

### 1) Ground Faults

For faults involving ground, the TD32 and 32V elements ensure reliable indication of the fault direction. These elements have been shown to be safe for the events evaluated and have high sensitivity for detecting high-impedance ground faults.

The TD32 element is directly associated with the directional comparison teleprotection scheme for sending the permissive signal. The POTT scheme uses a current-supervised TD32 element (TD67) for tripping. Likewise, the POTT scheme uses a zero-sequence current-supervised 32V element (67G) to send permissive signal and for tripping.

Even given the low fault contribution of the wind farm, the connection of the wind farm's step-up transformer (34.5/500 kV) allows it to contribute with zero-sequence current through the wind farm terminal for line faults.

### 2) Phase-to-Phase and Three-Phase Faults

For phase-to-phase faults (2P) without ground involvement, the TD32 element will also be employed to indicate the direction of the faults.

As shown in Section III, the use of the negative sequence can result in safety and reliability problems given the contribution of the IBR terminal, but its use is desirable for identification of the direction for faults between phases without ground involvement, since the 32V element is unavailable to assist in this case.

Reference [9] suggests a strategy for applying the 32Q function in this type of system. This strategy consists of defining a setting for the forward and reverse fault supervision overcurrent elements (50FP and 50RP, respectively) of the 32Q function with a threshold high enough to guarantee the security of these elements.

In this application, at the IBR terminal, 50FP and 50RP are set so that 32Q is enabled only for reverse faults. At the GRID terminal, 50FP and 50RP are set so that 32Q is enabled for line faults. These settings allow the elements to be enabled by the GRID contribution current only, where the relationship between  $V_2$  and  $I_2$  is coherent with the fault direction. Since the IBR contribution is limited, this strategy allows the function to have the sensitivity to detect reverse unbalanced faults at the IBR terminal, increasing the security of the hybrid POTT scheme that uses weak infeed and echo logic.

For the Main 2 relay, when 50FP is not activated, the fault-type identification function stops comparing the phasors of  $I_0$  and  $I_2$  and switches to a voltage-based faulted phase identification logic if the weak infeed logic is enabled, which is reliable for terminals with a weak source [9]. Therefore, proper setting of the 50FP is doubly beneficial in this IED. In addition to fault location, fault-type signaling, and single-pole trip, FID logic in this IED also supervises distance elements.

Additionally, the 32P-1 element works independently and is always available for phase-to-phase faults. As with the phase directional element with a quadrature connection, there can be a conflict between 32P-1 elements of different phases in faults like Case 2 of Section III. Adding 67G and 67Q supervision in the pilot protection scheme improves security in this case.

In the Main 2 IED, the 32Q element has priority over the 32P-2 element. When 32Q is not enabled, per the setting

strategy presented above, 32P-2 is also available for unbalanced phase-to-phase faults.

For three-phase faults (3P), the TD32, 32P-1 and 32P-2 elements are available. Reference [1] shows that 32P may lose security for 3P GRID faults and [9] suggests an enhanced 32P that can be implemented by current supervision and simple logic. This enhanced 32P element is used to supervise all phase elements.

The POTT scheme uses current-supervised 32Q (67Q) and 32P-1 or 32P-2 elements (67P) to send the permissive signal and for tripping. At the PV terminal, these elements do not operate for a line fault with the 50FP setting strategic presented above and trip at this terminal is based on weak infeed and echo-converted-to-trip (ECTT) logic. In the Main 1 relay, the weak infeed logic can be triggered by phase undervoltage (27P), negative-sequence overvoltage (59Q), or zero-sequence overvoltage (59G). In the Main 2 relay, phase-to-phase (27PP) and 59G are available

For both 2P and 3P elements, the TD32 element has the sensitivity to quickly identify and declare forward faults, even with the low magnitude of the IBR contribution, as discussed in [20]. The way TD32 is implemented in the POTT scheme in [22] requires current supervision for TD32 (TD67) only for tripping and not for sending the permissive signal. In the case of an internal fault, both terminals will send the permissive signal; however, only the GRID side will have enough current to trip by the POTT. To ensure a fast trip at the IBR side, it is necessary to use a DTT.

### B. Line Current Differential Protection

The Main 2 relay has a line differential function based on the alpha plane, providing phase differential elements (87LA, 87LB, and 87LC), a negative-sequence differential element (87LQ), and a zero-sequence differential element (87LG).

As shown in Section III, all these elements remain safe for external faults. Even with the unexpected behavior of  $I_2$  from the IBR terminal, the same current passes through both line terminals in the event of external faults. Thus, all differential elements can be enabled. Reference [9] also evaluates the security and reliability of 87L function for IBR connecting transmission lines.

### C. Distance and Step Distance Protection

As mentioned previously, the application of the distance function at the wind farm terminal leads to safety and reliability issues. An instantaneous Zone 1 element may overreach for external faults, and a time delay Zone 2 element may not be able to provide backup for the system due to the variation in the apparent impedance.

The enhanced 32P element can supervise phase distance elements at both line terminals. Additionally, to prevent Zone 1 overreaching, the phase Zone 1 element can be limited using the distance element overcurrent supervision or adding a time delay; these two conditions can also be combined in an OR gate. Adding a dropout delay in the Zone 2 element can avoid element dropout, providing dependable backup. All these solutions are suggested and detailed in [9].

Since the connection between the wind farm and the GRID is radial in this system, a distance element with an extended Zone 1 can be applied to the GRID terminal relay, with a reach beyond the 500 kV bus of the wind farm, as shown in Fig. 25. This increases instantaneous coverage for line faults, especially in the event of communications channel failures. Additionally, at the GRID terminal, the TD21 element can be applied with a reach near to the remote bus.

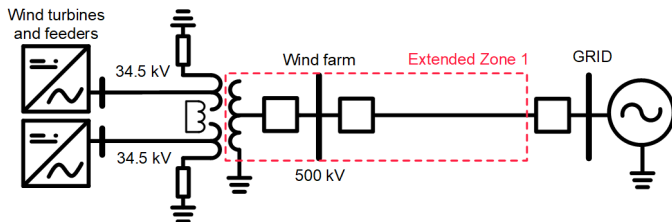


Fig. 25. Extended Zone 1 improves instantaneous coverage for line faults.

This strategy cannot be applied if more equipment (transmission lines or transformers) gets connected to the 500 kV bus of the wind farm terminal in the future.

For these faults, the current that passes through the line terminals is the current coming from the system, which is mostly composed of synchronous machines; therefore, the distance functions can operate normally.

#### D. TW-Based Features

Faults in the transmission line generate voltage and current transients that propagate toward the line terminals. When an incident wave ( $i_i$ ) reaches the line terminal, part is transmitted ( $i_T$ ) and part is reflected ( $i_R$ ), as shown in Fig. 26 [24].

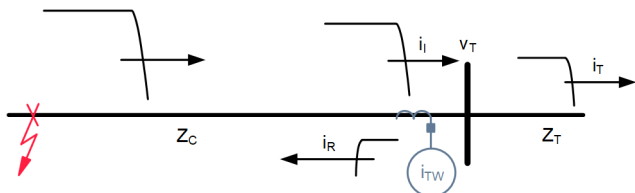


Fig. 26. Representation of incident ( $i_i$ ), reflected ( $i_R$ ), and transmitted ( $i_T$ ) waves at a transmission line terminal.

The portion of the wave that is reflected and transmitted depends on the ratio between the line's characteristic impedance ( $Z_C$ ) and the equivalent terminal impedance ( $Z_T$ ), which can be determined using (5) and (6).

$$i_R = \frac{Z_C - Z_T}{Z_C + Z_T} i_i \quad (5)$$

$$i_T = \frac{2 \cdot Z_C}{Z_C + Z_T} i_i \quad (6)$$

An IED that monitors the current signal at the line terminal sees the sum of the incident and reflected currents ( $i_{TW}$ ) according to (7).

$$i_{TW} = i_i + i_R \quad (7)$$

At the GRID terminal, two other transmission lines are connected, so  $Z_T$  is smaller than  $Z_C$ . This causes  $i_R$  to have the same polarity as  $i_i$  and causes  $i_{TW}$  to have a magnitude greater than the incident wave, which makes it easier to detect.

However, the termination of the line at the IBR is through a transformer, which means that  $Z_T$  has a much higher value compared to  $Z_C$ . This causes  $i_R$  and  $i_i$  to have opposite polarities and causes  $i_{TW}$  to have a magnitude smaller than the incident wave, which makes it difficult to detect.

Reference [25] shows actual records of current TWs in a transformer termination made by a TW-based fault-locating device in a configuration similar to the system studied here. The experience of this real system shows that, despite the attenuation in the magnitude, detection is still possible. Since the magnitude of the TW signal generated in the fault depends on the voltage incidence angle, the signal attenuation at the wind farm terminal reduces the sensitivity of TW-based functions, especially for faults that occur far from the voltage peak.

In the system in analysis, it will be applied using the following TW-based functions:

- TW-based directional element (TW32)
- TW-based line differential element (TW87)
- TW-based fault location with data from two terminals (DETWFL) [25]
- Predictive line monitoring based on TWs [26]

In cases when the IBR terminal is connected to more transmission lines, the low impedance increases the reliability of the TW functions.

#### E. Line Protection System Reliability

Most of the protection strategies described are dependent on the availability of the communications channel between the line terminals, excluding the distance elements. Therefore, to ensure the availability of the protection system, the means of communication must be highly available and redundant.

This becomes even more critical in applications when other transmission lines are connected to the IBR bus or more than one transformer, since the strategy of extending the reach of Zone 1 is not fully applicable.

The National Electric System Operator (ONS) of Brazilian grid requires, at a minimum, the total redundancy of the communications channel for all facilities with a voltage level equal to or greater than 230 kV.

Usually, transmission lines, especially newer ones, have an OPGW cable, which provides a reliable communications channel for both 87L protection and pilot protection schemes, either via direct fiber or through multiplexers.

To provide redundancy, an alternative route through nearby substations is an option. In this case, for radially connected IBRs, alternative routes are unlikely to be available. Communication redundancy can be obtained through a second OPGW cable, power line carrier (PLC), or spread-spectrum radios for short lines. These last two means of communication do not support or ideally meet the requirements of the 87L function [27], making it difficult to adopt the 87L function with full redundancy.

Thus, pilot protection using a directional comparison scheme is the natural alternative for these communications channels. The use of the TD32 function in the pilot protection

scheme, as detailed previously, increases dependability for fast elimination of internal faults in this type of system.

For GRID terminal bus faults and adjacent line faults, it is more challenging to provide remote backup with the wind farm terminal IED. The use of redundant local protection methods, including bus and circuit breaker failure protection, should be considered. The ONS's minimum requirement is redundancy for all these protection schemes in facilities with a voltage greater than or equal to 230 kV.

In the event of a total failure of communication with the GRID terminal, it might not be possible to eliminate the fault at the wind farm terminal. In this case, [9] suggests the use of a long-time undervoltage element for backup. Enabling the 27P element or even a distance function only when the two communications channels are lost is an alternative that should be evaluated.

## VI. CONCLUSION

This paper evaluated how an inverter-based source's atypical behavior and characteristics challenge the actual phasor-based protective functions, including symmetrical-components-based directional elements, fault-type identification logic, and distance elements. Field data from a 138 kV transmission line connecting a 420 MW PV to the GRID were evaluated, and the issues related to IBR's fault current contribution behavior were discussed.

Additionally, the data from the events were used to evaluate the performance of improved phasor-based and new time-domain protective features presented in modern protection relays. These elements proved to be more secure and reliable for these systems.

The TD32 element was reliable for the evaluated field cases. The use of this element in a directional comparison pilot protection scheme could improve the protection reliability.

The 87L function was secure for the evaluated events and was also presented as an excellent protection scheme for the IBR connecting transmission lines in previous papers; however, two redundant and independent communication channels suitable for 87L are not always available. A directional comparison pilot protection scheme was more flexible in terms of the communication channel requirements and allowed the deployment of a fully redundant protection system for these systems when applied with TD32.

A protection philosophy combining phasor-based elements and time-domain incremental quantities was proposed, based on the validation made with field data in the conclusion of this paper and previous papers. This protection philosophy will be applied in the transmission line connecting the new wind farm that is currently in the design stage.

Considerations about transmission line protection system and system backup protection reliability were discussed. Brazilian grid protection system minimum requirements were also accounted for.

Finally, the use of TW-based protection features to protect the transmission lines connecting IBR is in the authors' interest and will be evaluated for the new wind farm enterprise in Brazil.

## VII. ACKNOWLEDGMENT

The authors acknowledge Ritwik Chowdhury and Ryan McDaniel of Schweitzer Engineering Laboratories, Inc. (SEL) for their time spent reviewing this paper and having technical discussions.

## VIII. REFERENCES

- [1] R. Chowdhury and N. Fischer, "Transmission Line Protection for Systems With Inverter-Based Resources – Part I: Problems," *IEEE Transactions on Power Delivery*, August 2020. Available: doi.org/10.1109/TPWRD.2020.3019990.
- [2] B. Kasztenny, N. Fischer, and H. Altuve, "Negative-Sequence Differential Protection – Principles, Sensitivity, and Security," proceedings of the 41st Annual Western Protective Relay Conference, College Station, TX, October 2014.
- [3] K. Zimmerman and J. Mooney, "Comparing Ground Directional Element Performance Using Field Data," proceedings of the 8th Annual Conference for Fault and Disturbance Analysis, College Station, TX, April 1993.
- [4] R. Abboud, P. Lima, and A. Pontizelli, "Utilização de IEC 61850 Valores Amostrados (SV) e Sincrofasores para Localização de Faltas em Tempo Real," proceedings of the Symposium of Experts in Operation Planning and Electric Expansion, Foz do Iguaçu, Paraná, Brazil, May 2014.
- [5] N. Fischer, D. Finney, and D. Taylor, "How to Determine the Effectiveness of Generator Differential Protection," proceedings of the 40th Annual Western Protective Relay Conference, College Station, TX, October 2013.
- [6] D. Costello and K. Zimmerman, "Determining the Faulted Phase," proceedings of the 36th Annual Western Protective Relay Conference, College Station, TX, October 2009.
- [7] F. Calero, "Rebirth of Negative-Sequence Quantities in Protective Relaying With Microprocessor-Based Relays," proceedings of the 30th Annual Western Protective Relay Conference, College Station, TX, October 2003.
- [8] W. Elmore, *Protective Relaying Theory and Applications*, Marcel Dekker, Inc., New York, NY, 1994.
- [9] R. Chowdhury and N. Fischer, "Transmission Line Protection for Systems With Inverter-Based Resources – Part II: Solutions," proceedings of the IEEE Transactions on Power Delivery, Virtual Format, October 2020. Available: ieeexplore.ieee.org/document/9233925.
- [10] Ministry of Mines and Energy, "Resenha Energética Brasileira," March 2020. Available: antigo.mme.gov.br/web/guest/secretarias/planejamento-e-desenvolvimento-energetico/publicacoes/resenha-energetica-brasileira.
- [11] E. Senger and F. Filho, "Plantas eólicas: modelagem para estudos de curto-circuito e critérios de ajustes das proteções," proceedings of the Protection and Control Technical Seminar, Rio de Janeiro, Brazil, 2014.
- [12] M. Nunes, "Avaliação do comportamento de aerogeradores de velocidade fixa e variável integrados em redes elétricas fracas," PhD dissertation, UFSC Institutional Repository, 2003. Available: repositario.ufsc.br/xmlui/handle/123456789/85795.
- [13] E. Pinheiro, "Análise do Comportamento Dinâmico de Usinas Eólicas a Velocidade Variável Utilizando ATPDraw," PhD dissertation, Federal University of Minas Gerais, 2004.
- [14] J. Marques, "Turbinas eólicas: modelo, análise e controle do gerador de indução com dupla alimentação," PhD dissertation, Federal University of Santa Maria, 2004.
- [15] B. Kasztenny, V. Mynam, and N. Fischer "Sequence Component Applications in Protective Relays – Advantages, Limitations, and Solutions," proceedings of the 46th Annual Western Protective Relay Conference, Spokane, WA, October 2019.
- [16] ABB, "Technical Application Papers No. 10: Photovoltaic Plants," Available: abb.com.

- [17] J. Roberts and A. Guzmán, “Directional Element Design and Evaluation,” proceedings of the 21st Annual Western Protective Relay Conference, Spokane, WA, October 1994.
- [18] B. Fleming, “Negative-Sequence Impedance Directional Element,” proceedings of the 10th Annual ProTest User Group Meeting, Pasadena, CA, February 1998.
- [19] J. Roberts, D. Tziouvaras, G. Benmouyal, and H. Altuve, “The Effect of Multiprinciple Line Protection on Dependability and Security,” proceedings of the 55th Annual Georgia Tech Protective Relaying Conference, Atlanta, GA, May 2001.
- [20] B. Kasztenny, “Distance Elements for Line Protection Applications Near Unconventional Sources,” June 2021. Available: selinc.com.
- [21] E. O. Schweitzer, III, B. Kasztenny, A. Guzmán, V. Skendzic, and V. Mynam, “Speed of Line Protection – Can We Break Free of Phasor Limitations?” proceedings of the 41st Annual Western Protective Relay Conference, Spokane, WA, October 2014.
- [22] *SEL-T401L Ultra-High-Speed Line Relay Instruction Manual*. Available: selinc.com.
- [23] E. O. Schweitzer, III, and B. Kasztenny, “Distance Protection: Why Have We Started With a Circle, Does It Matter, and What Else Is Out There?” proceedings of the 71st Annual Conference for Protective Relay Engineers, College Station, TX, March 2018.
- [24] A. Guzmán, B. Kasztenny, Y. Tong, and V. Mynam, “Accurate and Economical Traveling-Wave Fault Locating Without Communications,” proceedings of the 71st Annual Conference for Protective Relay Engineers, College Station, TX, March 2018.
- [25] E. O. Schweitzer, III, A. Guzmán, V. Mynam, V. Skendzic, B. Kasztenny, and S. Marx, “Locating Faults by the Traveling Waves They Launch,” proceedings of the 67th Annual Conference for Protective Relay Engineers, College Station, TX, April 2014.
- [26] B. Kasztenny, V. Mynam, T. Joshi, and D. Holmbo, “Preventing Line Faults With Continuous Monitoring Based on Current Traveling Waves,” proceedings of the 15th International Conference on Developments in Power System Protection Liverpool, United Kingdom, March 2020.
- [27] B. Kasztenny, N. Fischer, K. Fodero, and A. Zvarych, “Communications and Data Synchronization for Line Current Differential Schemes,” proceedings of the 2nd Annual Protection, Automation, and Control World Conference, Dublin, Ireland, June 2011.

## IX. BIOGRAPHIES

**Marcelo Bini** received his BSEE in electrical engineering from Santa Catarina State University (Joinville campus), Brazil, in 2006. In 2006, he joined Engevix Engineering as an electrical engineer, working with hydroelectric power plant projects with emphasis on protection, control, and measurement systems. In 2017, he joined Araxá Solar as a substation design engineer. In 2019, he joined EDF Renewables as an electrical engineer, working with protection and control design and other electrical projects involved in substations, transmission lines, and medium voltage networks.

**Ricardo Abboud** received his BSEE degree in electrical engineering from Federal University of Uberlândia, Brazil, in 1992. In 1993, he joined CPFL Energia as a protection engineer. In 2000, he joined Schweitzer Engineering Laboratories, Inc. (SEL) as a field application engineer in Brazil, assisting customers in substation protection, automation, and control systems. In 2005, he became the field engineering manager, leading and mentoring the application engineering group, and in 2014, he became the engineering services manager. In 2016, he transferred to SEL headquarters in Pullman, Washington, as an international technical manager, providing advanced technical support and consultancy about new technologies to international field offices. In 2019, he joined SEL University as a professor. Currently, he is a principal engineer with SEL Engineering Services, Inc. (SEL ES).

**Paulo Lima** received his BSEE in electrical engineering from Federal University of Itajubá, Brazil, in 2012. In 2013, he joined Schweitzer Engineering Laboratories, Inc. (SEL) as a protection application engineer in Brazil. In 2018, he became an application engineering group coordinator, and he has been the regional technical manager for Brazil since 2020. He has experience in application, training, integration, and testing of digital protective relays. He also provides technical writing and training associated with SEL products and SEL University.

**Fabio Lollo** received his BSEE in electrical engineering from São Paulo State University (Bauru campus), Brazil, in 1997. In 1998, he joined BMG Engineering as an electrical engineer, working with protection and control design and protection studies. In 2013, he joined Schweitzer Engineering Laboratories, Inc. (SEL) as senior protection engineer in Brazil. In 2016, he became design and studies group coordinator. Currently, he is a senior protection engineer and supervises a group of project engineers with SEL Engineering Services, Inc. (SEL ES). He has experience in short circuit calculation and protection settings for industrial and utility systems.